Available online at www.sciencedirect.com
ScienceDirect
Journal of Hazardous Materials 154 (2008) 245–253
Journal of Hazardous Materials
www.elsevier.com/locate/jhazmat

Photocatalytic degradation of methyl red dye by silica nanoparticles

Y. Badr [a], M.G. Abd El-Wahed [b], M.A. Mahmoud [b,*]

[a] National Institute of Laser Enhanced Science, Cairo University, Cairo, Egypt
[b] Chemistry Department, Faculty of Science, Zagazig University, Zagazig, Egypt

Received 3 July 2006; received in revised form 9 October 2007; accepted 10 October 2007
Available online 13 October 2007

Abstract

Silica nanoparticles (SiO_2 NPs) were found to be photocatalytically active for degradation of methyl red dye (MR). The SiO_2 NPs and SiO_2 NPs doped with silver (and or) gold nanoparticles were prepared. From the transmission electron microscopy (TEM) images the particle size and particle morphology of catalysts were monitored. Moreover, SiO_2 NPs doped with silver and gold ions were used as a photocatalyst for degradation of MR. The rate of photocatalytic degradation of MR was found to be increased in the order of SiO_2 NPs, SiO_2 NPs coated with gold nanoparticles (Au NPs) and silver nanoparticles (Ag NPs), SiO_2 NPs coated with Ag NPs, SiO_2 NPs coated with Au NPs, Ag^+-doped SiO_2 NPs, and Au^{3+}-doped SiO_2 NPs. The kinetic and mechanism of photocatalytic reaction were studied and accorded well with experimental results.

Keywords: Silica nanoparticles; Photocatalysis; Photodegradation; Gold; Silver

1. Introduction

Most of the dyes used in dying textile, paper, leather, ceramic, cosmetics, ink, food processing are azo dyes, which are characterized by the presence of one or more azo group (–N=N–) in their structure [1]. Moreover, 15% of the dyes produced worldwide are lost during synthesis and processing with wastewater [2]; these dyes were found to have great hazards on the human health and the environment due to their toxicity [3,4]. It is well known that methyl red dye has been used in textile dying and paper printing [5]; however, it causes eye and skin irritation and digestive tract if inhaled/swallowed. There are several methods for pollutant treatment which involve chemical, physical, and biological processes. The chemical methods include chlorination and ozonation [6]. While, the physical methods depend on the removal of the pollutant without degradation such as reverse osmosis, flocculation, membrane filtration and adsorption on activated charcoal [7–9]. Finally, the biological methods depend mainly on biodegradation of the pollutant [10,11], but bacterial beds degradation is less effective due to the fluctuations of the wastewater composition [12]. Furthermore, bio-treatment of azo dyes is less adapted [13,14] because of their resistance to aerobic degradation and by anaerobic degradation carcinogenic aromatic amines could be formed.

Although silica is basically inert for many reactions, it shows noticeable activities towards some catalytic [15–17]. Pure silica was proven to remote photocatalytic reactions under UV irradiation, e.g. photo-oxidation of CO [18], photo-metathesis of propene [19,20], and photo-epoxidation of propene [21]. Silica-based photocatalysts have been used and exhibit activity under UV irradiation at room temperature, such as silica–alumina [22,23], silica-supported zirconia [24], and silica–alumina–titania [25].

The photoactive sites were formed on the surface of SiO_2 prepared by sol–gel method [21]; these active sites were revealed by VUV-UV, IR, ESR, and photoluminescence spectroscopy [26]. The IR symmetric stretching vibration of the $Si{-}O^-$ non-bridging bond appeared at 950 cm^{-1}. Moreover, The enhancement of the peak intensity at 950 cm^{-1} indicates an increase in the amount of the non-bridging oxygen, i.e. a change in the structural units from SiO_2 (three-dimensional network structure) to SiO_4 (isolated tetrahedron) [27]. The SiO_2 NPs can be photoexcited under UV light below ~390 nm, which corresponds to a charge transfer (258 nm wavelength) from bonding

* Corresponding author.
E-mail address: mahmoudchem@yahoo.com (M.A. Mahmoud).

0304-3894/$ – see front matter © 2007 Elsevier B.V. All rights reserved.
doi:10.1016/j.jhazmat.2007.10.020

orbital of Si–O to 2p non-bonding orbital of non-bridging oxygen [28].

The photoluminescence spectra of silica are resolved into four Gaussian peaks at approximately 2.5, 2.8, 3.0, and 3.2 eV. The luminescence band near 2.5 and 2.8 eV is associated with the decay in the self-trapped exciton as a pair of a hole localized on oxygen and an electron on the neighboring silicon in the silica matrix [29,30]. While, the bands at 3.0 and 3.2 eV are induced by the electron–hole recombination at the unknown oxygen-deficient-associated defect centers [31,32].

When the metal ions present with the semiconductor photocatalyst, a considerable controversy on the effect of metal ions was observed; they act as a rate accelerator [33,34], while on other cases the rate was found to decrease upon the addition of metal ions [35,36].

The present work aims to prepare silica nanoparticle and modify its surface by doping with metal ions or coating with other metallic nanoparticles, and finally study the effect of additives on the kinetic and mechanism of photocatalytic degradation of MR dye.

2. Experimental

2.1. Materials and methods

Methyl red (MR), ethanol, and tetraethylorthosilicate (TEOS), purchased from Sigma–Aldrich, were used, while silver nitrate ($AgNO_3$), nitric acid (HNO_3), hydrogen tetrachloroaurate ($HAuCl_4$), and sodium borohydride ($NaBH_4$) were obtained from Fluka.

2.1.1. Preparation of silica nanoparticles (SiO_2 NPs)

The silica nanoparticles (SiO_2 NPs) were prepared from TEOS by HNO_3 as an acid catalyst [37]. TEOS and ethanol with volumes of 10 mL were mixed together; the resulting mixture was added drop by drop in 60 mL 0.1N HNO_3 solution; the final mixture was stirred for 8 h at 60 °C for complete hydrolysis of TEOS to SiO_2 NPs. The concentration of SiO_2 NPs solution was found to be (30 g/L) after it was completed to 90 mL by distilled water. These particles were centrifuged and washed with ethanol and dried in air. These particles are used without any further treatment for coating or catalysis.

2.1.2. Preparation of SiO_2 doped with Ag^+ or Au^{3+}

SiO_2 NPs doped with 0.1% Ag^+ or Au^{3+} ion were prepared by mixing 10^{-3} M of $AgNO_3$ or $HAuCl_4$ with 0.999 M SiO_2 NPs in 100 mL of double distilled water and stirring it thoroughly. The solution was then allowed to stand for 2 h to allow the ions to be adsorbed completely [38]. The resulting particles were dried under vacuum until complete dryness, and then dried in air.

2.1.3. Preparation of Ag NPs (and, or) Au NPs deposited on the surface of SiO_2 NPs

Ag NPs or Au NPs deposited on the surface of SiO_2 NPs with molecular ratio of 0.1% was prepared by mixing 10^{-3} M of $AgNO_3$ or $HAuCl_4$ with 0.999 M SiO_2 NPs in 80 mL of double distilled water and stirring vigorously for 5 min. Then 10^{-3} M $NaBH_4$ was added and the solution was completed to 100 mL by double distilled water [39]. To prepare Au NPs and Ag NPs composite deposited on the surface of SiO_2 NPs, the 5×10^{-4} M of $AgNO_3$ was mixed with 0.999 M and the solution was stirred for 5 min; then 5×10^{-4} mol $NaBH_4$ was added. Thereafter 5×10^{-4} M of $HAuCl_4$ was added followed by stirring and 5×10^{-4} M $NaBH_4$ addition. Following the reduction the samples were repeatedly centrifuged and washed with water to remove non-reacted $AgNO_3$ and $HAuCl_4$, and then dried at 80 °C.

2.1.4. Photocatalytic degradation experiment

The photocatalyst SiO_2 NPs, SiO_2 NPs doped with Ag^+ or Au^{3+}, and Ag NPs (and, or) Au NPs deposited on the surface of SiO_2 NPs was added to MR solution to obtain 100 mL of 500 mg/L photocatalyst and 50 ppm of MR. Then, to establish the adsorption equilibrium between the MR and the photocatalysts, the resulting solution was stirred in dark for 20 min. Thereafter, the zero time reading was taken and the solution was exposed to the Xenon lamp. Before the measurements of absorption, the samples of the examined solutions were centrifuged (20 min at 5000 rpm) to remove the catalysts which were coagulated.

2.2. Instruments

The set-up used for photocatalytic degradation experiment consists of a 250 mL beaker and 20 cm above it a Xenon lamp (50 W) (Orial mode 66001) was used as an artificial sunlight source. Moreover, the beaker stirred by a magnetic stirrer during the irradiation as shown in Fig. 1.

Bio-carry 50 UV-Vis spectrophotometer with range of 190–1100 nm was used to measure the UV–vis absorption spectra of MR as function of irradiation time. Transmission electron microscopy (TEM) (JEOL) was used to determine the particle size and morphology. TEM photographs were taken by drying a drop of colloidal photocatalyst on a surface of copper-coated

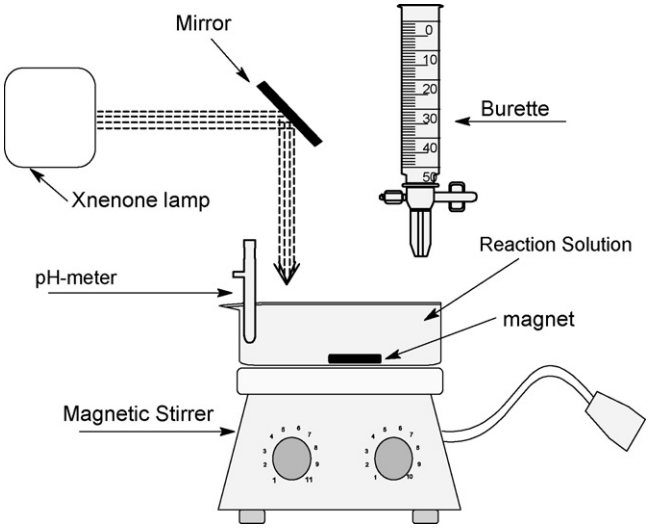

Fig. 1. Schematic diagram for the photoreactor set-up.

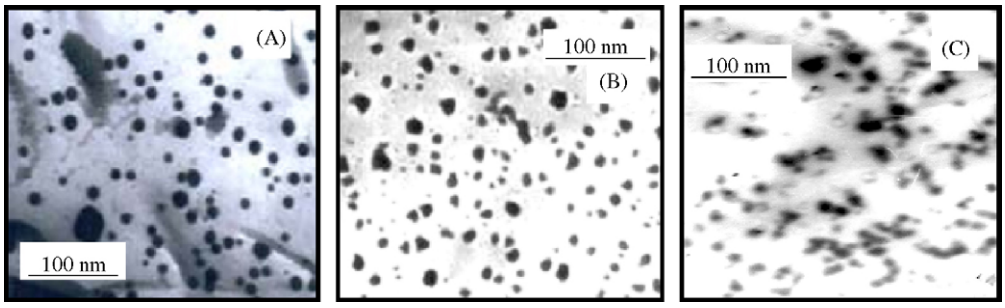

Fig. 2. Transmission electron microscopy (TEM) photographs of (A) SiO_2 NPs and (B, C) Ag NPs and Au NPs deposited on the surface of SiO_2 NPs.

carbon grid, which has undergone TEM photography. Moreover, the particle size and distribution were measured as follows: 150 particles were enlarged on the TEM photography and their sizes were measured, then the distribution was obtained from statistical calculation.

MR dye has absorption maximum at 522 nm at pH ~4 and its concentration can be determined spectrophotometrically with the aid of a calibration curve (a relationship between the dye concentration and its peak intensity at maximum absorption). The results revealed a linear relationship over all the dye concentrations, i.e. Beer's law is obeyed.

3. Results and discussion

3.1. Determination of the particle size of silica photocatalysts

The catalytic powers of the catalysts are strongly correlated with their particle size and distributions, because the particles size has a great effect on the energy levels of the nanophotocatalyst. Consequently, to obtain good understanding for the photocatalytic processes, the particle size, morphology, and size distribution of the photocatalyst should be studied. Fig. 2 represents the TEM photography of (a) SiO_2 NPs and (b, c) Ag NPs or Au NPs deposited on the surface of SiO_2 NPs. The SiO_2 NPs showed a spherical shape with large distribution (15 ± 8 nm), while in case of Ag NPs or Au NPs deposited on the surface of SiO_2 NPs an irregular shape was obtained due to the appearance of Ag NPs or Au NPs on the surface of SiO_2 NPs and the particles size was approximately (17 ± 5 and 19 ± 6 nm), respectively.

3.2. Photocatalytic degradation of MR dye by SiO_2 NPs

The absorption band of MR dye was found to be centered at 522 nm; no change in this absorption peak intensity was observed in dark until 10 h (in the presence or absence of SiO_2 NPs). Moreover, a very small change in the intensity of maximum absorption was observed in the absence of SiO_2 NPs even after 120 min irradiation.

Fig. 3 shows the absorption spectra of MR before and after exposure to Xenon lamp at different timescale in the presence of SiO_2 NPs as a photocatalyst; the intensity of peak was found to decrease by increasing the irradiation time due to photocatalytic degradation of dye by SiO_2 NPs. On the other hand, the intensity of a peak at ~415 nm appeared to increase with time up to 50 min, then decrease again. Furthermore, the complete decolorization of the solution was obtained after 120 min.

3.3. Photocatalytic degradation of MR dye by Ag NPs (and, or) Au NPs deposited on the surface of SiO_2 NPs

The Ag and Au nanoparticles have a great effect on the catalytic properties of SiO_2 NPs. The photocatalytic degradation of MR was done in the presence of Ag NPs and/or Au NPs deposited on the surface of SiO_2 NPs. Fig. 4 represents the spectra of the remaining MR after photocatalytic degradation by (a) Ag NPs deposited on SiO_2 NPs and (b) Au NPs deposited on SiO_2 NPs as a function of irradiation time. The band corresponding to MR absorption was found to be decreased with time in case of both Ag NPs deposited on SiO_2 NPs and Au NPs deposited on SiO_2 NPs, but the rate of decay in case of silver

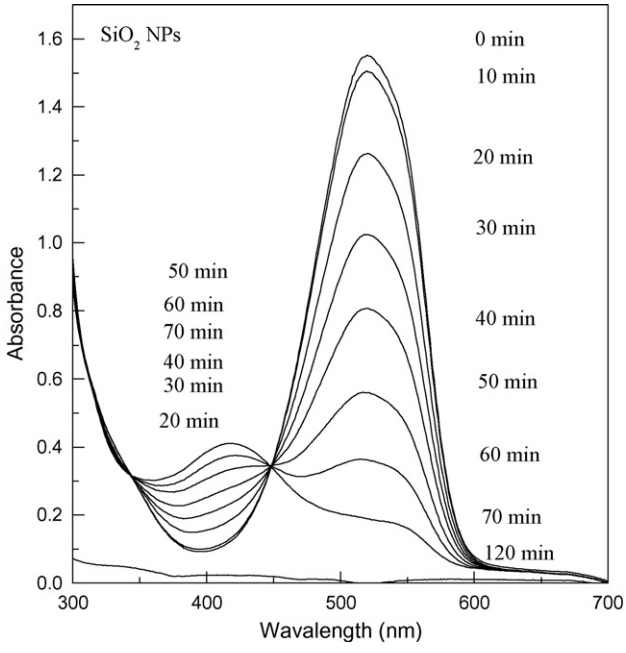

Fig. 3. The absorption spectra of methyl red after photocatalytic degradation by SiO_2 NPs after irradiation for different times.

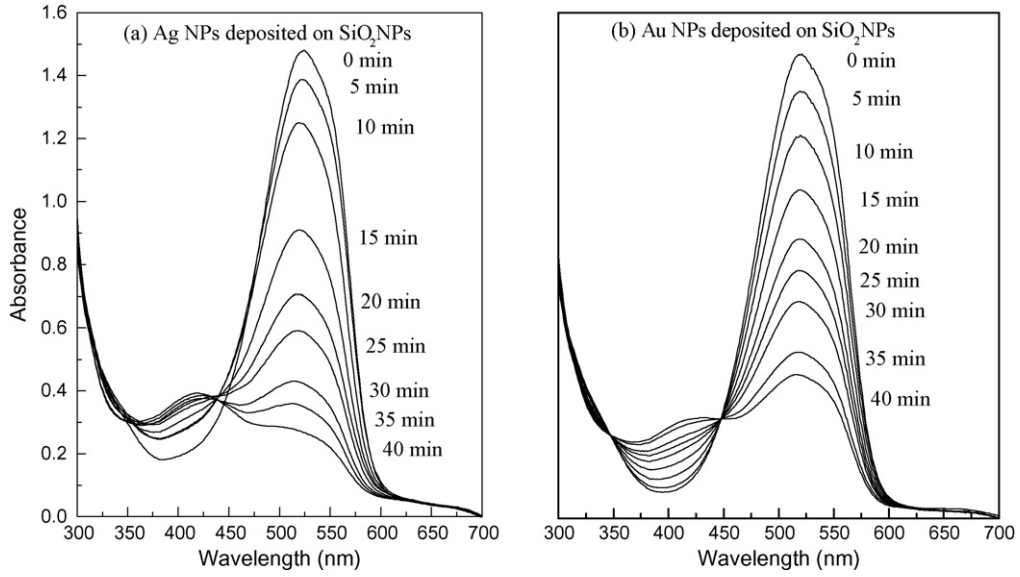

Fig. 4. The absorption spectra of methyl red after photocatalytic degradation by (a) Ag NPs deposited on SiO_2 NPs, (b) Au NPs deposited on SiO_2 NPs; after irradiation for different times.

appeared to be sharper than in case of gold. Both Ag NPs and Au NPs have rate of decay larger than pure SiO_2 NPs as shown in Fig. 3. On the other hand, the rate of decay of MR peak in case of double deposition of Au NPs and Ag NPs on SiO_2 NPs catalyst lies in between pure Ag NPs and Au NPs deposited on the surface of SiO_2 NPs (see Fig. 5); consequently, the activity of SiO_2 increases by depositing on it either nanoparticles but the silver increases the decay more than gold. The complete decolorization takes place after 70, 90, and 75 min for Ag NPs deposited on SiO_2 NPs, Ag NPs deposited on SiO_2 NPs, and Au NPs and Ag NPs deposited on SiO_2 NPs catalyst, respectively. The intermediate products in case of Au NPs were found to be less than that in case of Ag NPs, but these products decreased after 35 min in the two cases.

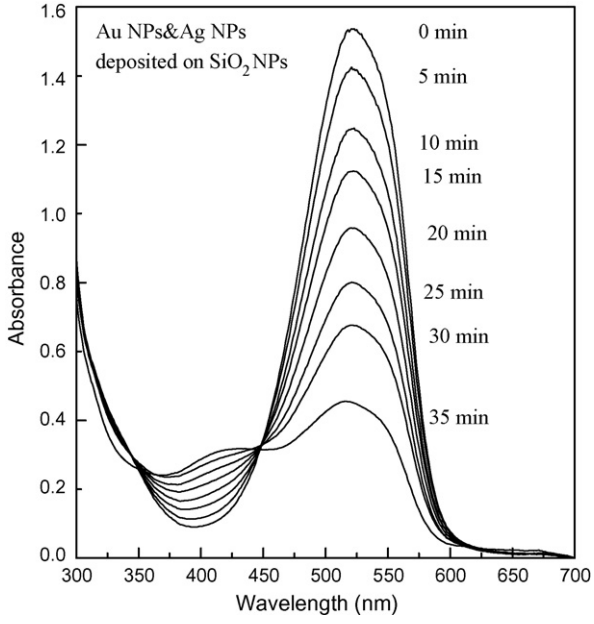

Fig. 5. The absorption spectra of methyl red after photocatalytic degradation by Au NPs and Ag NPs deposited on SiO_2 NPs after irradiation for different times.

3.4. Photocatalytic degradation of MR dye by SiO_2 NPs doped with Ag^+ and Au^{3+} ions

The photocatalytic degradation of MR by SiO_2 NPs was found to be enhanced in the presence of Ag^+ or Au^{3+} ions. Fig. 6 shows the spectra of the photocatalytic degradation of MR by SiO_2 NPs doped with silver ions (Ag^+), and SiO_2 NPs doped with gold ions (Au^{3+}) as a function of exposure time to the Xenon lamp. The rate of photocatalytic degradation of MR by SiO_2 NPs doped with Au^{3+} was observed to be fast in comparison with doping with Ag^+. Moreover, the rate is faster than in case of pure SiO_2 NPs, although the color of SiO_2 NPs becomes dark in case of silver and gold ions doping. The amount of intermediate products was found to be increased with time in case of doping with Ag^+ and Au^{3+} till 20 and 5 min, respectively, then decay till complete decolorization in 60 and 13 min, respectively.

3.5. Kinetics study of photocatalytic degradation

Langmuir-Hinshelwood model [40] can be used to describe the relationship between the rates of the photocatalytic degradation of dye in the presence of SiO_2 NPs as a function of irradiation time. The rate equation is used in the form [41]:

$$\frac{-\mathrm{d}C}{\mathrm{d}t} = \frac{k_{\text{L-H}} K_{\text{ad}} C}{1 + K_{\text{ad}} C} \tag{1}$$

where K_{ad} is the adsorption coefficient of the reactant on SiO_2, $k_{\text{L-H}}$ is the reaction rate constant, and C is the concentration at any time t. The values of $k_{\text{L-H}}$ and K_{ad} are used to explain the effect of light intensity on the equilibrium constant for fast adsorption–desorption processes between surface monolayer at

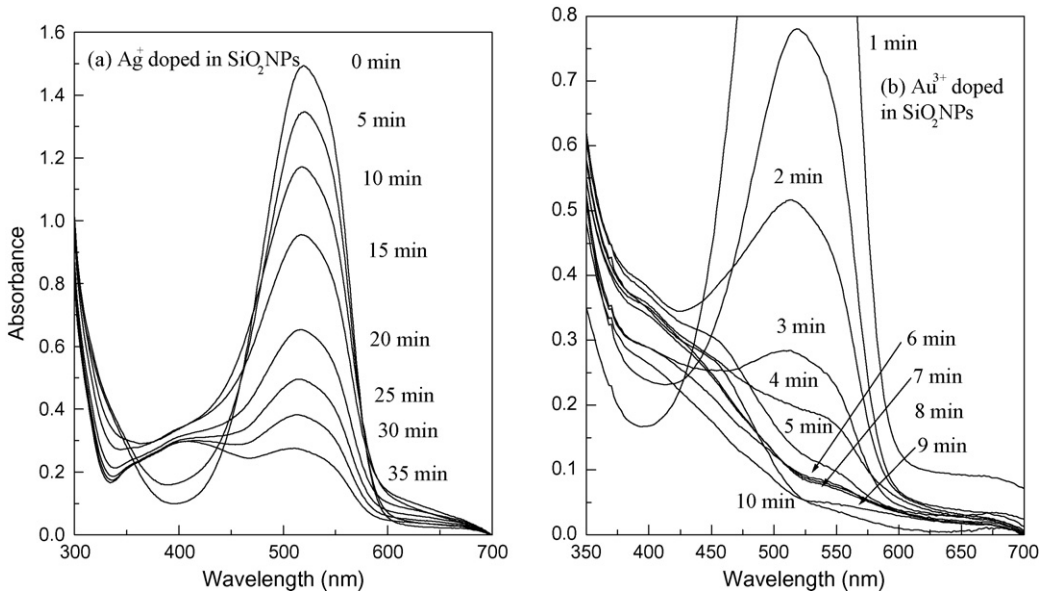

Fig. 6. The absorption spectra of methyl red after photocatalytic degradation by (a) SiO_2 NPs doped with silver ions (Ag^+), (b) SiO_2 NPs doped with gold ions (Au^{3+}); after irradiation for different times.

SiO_2 and bulk solution. Then, by integration of Eq. (1):

$$\ln\left(\frac{C_0}{C}\right) = K(C - C_0) + k_{\text{L-H}}K_{\text{ad}}t \tag{2}$$

where C_0 is the initial concentration.

For pseudo first-order reaction $K_{\text{ad}}C$ is very small as compared to 1 in the denominator of Eq. (1) so it simplified and integrated to be:

$$\ln\left(\frac{C_0}{C}\right) = k_{\text{L-H}}K_{\text{ad}}t = kt \tag{3}$$

where $k = k_{\text{L–H}}K_{\text{ad}}$ is the pseudo first-order reaction rate constant, and the half-life time $t_{(1/2)}$ can be calculated using the following expression:

$$t_{1/2} = \frac{0.693}{k} \tag{4}$$

Plotting the relation between the natural logarithm of the ratio between the original concentration of MR and the concentration after photocatalytic degradation ($\ln(C_0/C)$ versus the corresponding irradiation time (min) a linear relationship was obtained as shown in Fig. 7. Therefore, the photocatalytic degradation reaction of MR by SiO_2 NPs belong to the pseudo first-order reaction kinetics. The rate constant (slope in Fig. 7) and half-life time (Eq. (4)) were calculated and summarized in Table 1 the photocatalytic degradation of MR by SiO_2 NPs, SiO_2 NPs doped with Ag^+ ions, SiO_2 NPs doped with Au^{3+}ions, Ag NPs (and, or) Au NPs deposited on the surface of SiO_2 NPs.

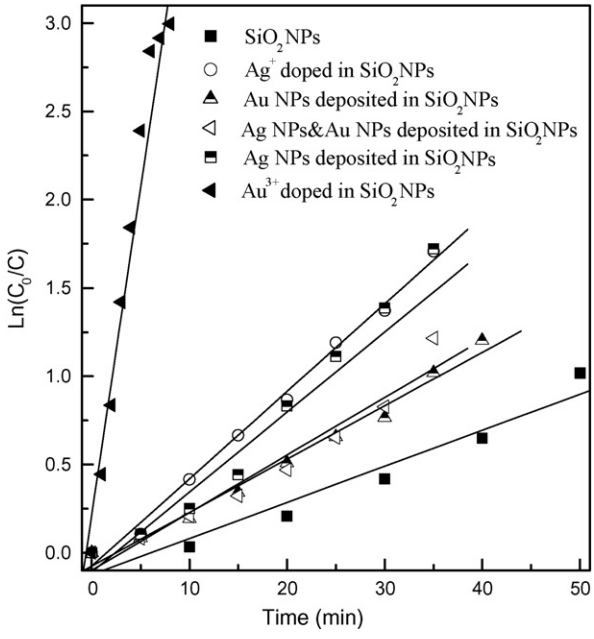

Fig. 7. The logarithm of the ratio between the original concentration of dye and the concentration after photocatalytic degradation by SiO_2 NPs, SiO_2 NPs doped with Ag^+ ions, SiO_2 NPs doped with Au^{3+}ions, Ag NPs (and, or) Au NPs deposited on the surface of SiO_2 NPs ($\ln(C_0/C)$) vs. the corresponding irradiation time (min).

Table 1
The rate constant and half-life time of some photocatalytic degradation of methyl red

Catalyst	Rate constant (min^{-1})	Half-life time (min)
Au^{3+} doped SiO_2 NPs	0.37	1.9
Ag^+ doped SiO_2 NPs	0.050	13.9
Ag NPs deposited SiO_2 NPs	0.046	15.1
Au NPs and Ag NPs deposited SiO_2 NPs	0.037	18.7
Au NPs deposited SiO_2 NPs	0.032	21.7
SiO_2 NPs	0.020	34.6

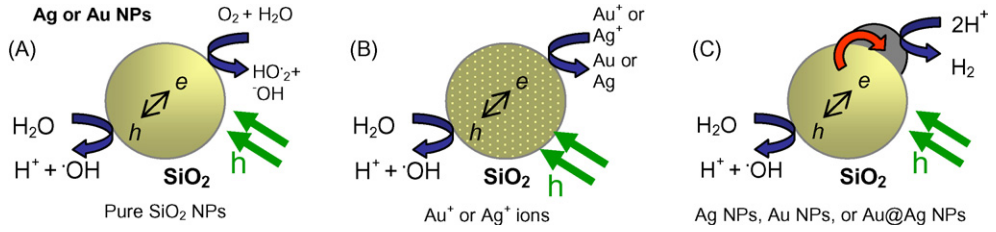

Fig. 8. The mechanism of photocatalytic effect of (A) SiO_2 NPs, (B) SiO_2 NPs doped with Ag^+ Au^{3+} ions, and (C) Ag NPs or Au NPs deposited on the surface of SiO_2 NPs.

3.6. The mechanism for photocatalytic degradation of MR dye

Jiang et al. [42] studied the negative shift in the X-ray photoelectron spectra of SiO_2 NPs coated with Ag NPs as compared with pure SiO_2 NPs and reported that this shift might be attributed to the electron transfer between Ag NPs and SiO_2 NPs. Moreover, SiO_2 NPs was found to be photoexcited under UV irradiation and showed an absorption band at around 309 nm, which is attributed to the charge transfer from bonding orbital of Si–O to 2p non-bonding orbital of non bridging oxygen [43].

When a photon of UV light strikes the SiO_2 surface, an electron from its valence band (vb) jumps to conduction band (cb) generating a positively charged hole in the valence band (h_{vb}^+), while the negative charge is increased in the conduction band (e_{cb}^-) and photocatalytic active centers will be formed on the surface of SiO_2 NPs (as proven from the photoluminescence measurements) [29–32] according to the Eq. (5):

$$SiO_2 + h\nu \rightarrow e_{cb}^- + h_{vb}^+ \quad (5)$$

The valence band holes thus formed react with the chemisorbed H_2O molecules to form reactive species such as $^\bullet$OH radicals, which attack dye molecules successively to cause their complete degradation.

$$(H_2O \rightarrow H^+ + OH^-) + h_{vb}^+ \rightarrow H^+ + {}^\bullet OH \quad (6)$$

On the other side, e_{cb}^- and h_{vb}^+ can recombine on the surface of the particle within few nanoseconds and the resulting energy dissipated as heat. Furthermore the e_{cb}^- and the h_{vb}^+ can be trapped in surface states where they can react with adsorbed species or close to the surface of the particle. The e_{cb}^- could react with acceptor, e.g. dissolved O_2, which consequently is transformed into super oxide radical anion ($O_2^{\bullet -}$) leading to the additional formation of $^\bullet O_2H$ as given in Eq. (7).

$$O_2 + e_{cb}^- \rightarrow O_2^{-\bullet} + (H^+ + {}^-OH) \rightarrow HO_2^\bullet + {}^-OH \quad (7)$$

On the other hand, h_{vb}^+ could interact with donor, e.g. $^-$OH and $^\bullet O_2H$ forming $^\bullet$OH radical which attack the MR in following manner.

$$HO_2^\bullet + {}^-OH + h_{vb}^- \rightarrow {}^\bullet OH \quad (8)$$

The main factor affecting the efficiency of SiO_2 NPs is the amount of $^\bullet$OH radicals as described above. Consequently any factor supports the generation of $^\bullet$OH radicals will enhance the rate of the photocatalytic degradation of MR. When Au^{3+} or Ag^+ ions present during the reaction they are absorbed on the surface of SiO_2 NPs then, combined with the electrons in the conduction band of SiO_2 NPs, forming the corresponding metal (Eq. (9)). It reduces the recombination of charges (h_{vb}^+ and e_{cb}^-) and favors the formation of $^\bullet$OH radical [44]. Therefore it was observed that the catalyst were slightly darkens during the irradiation. The oxidative pathway leads, in many cases, to complete mineralization of an organic substrate to CO_2 and H_2O. The enhancing effect of Au^{3+} and Ag^+ may be explained by their ability to trap electrons and generate holes so they act as electron scavengers [45].

$$e_{cb}^- + (Au^{3+}, Ag^+, \text{or } H^+) \rightarrow (Au^0, Ag^0, \text{or } H_2 \uparrow) \quad (9)$$

The mechanism of photocatalytic degradation of MR by surface of SiO_2 NPs loaded with Ag NPs, Au NPs and Ag NPs, or Au NPs could be controlled by the deposited nanoparticles which affect the electron–hole recombination process [46–49]. The major role of Ag NPs, Au NPs and Ag NPs, or Au NPs deposited on SiO_2 NPs is attributed to the consumption of the electrons and its transmission it to the H^+ ions or to O_2. Therefore the retardation of the electron–hole recombination will increase the photocatalytic efficiency of the SiO_2 NPs photocatalysts, and consequently accelerates hydroxyl radical formation and enhancing the degradation rate of MR initiated by $^\bullet$OH [50,51] Eqs. (10)–(12):

$$\text{Ag or Au} + e_{cb}^- \rightarrow \text{Ag}(e_{cb}^-)\text{or Au}(e_{cb}^-) \quad (10)$$

$$\text{Ag}(e_{cb}^-)\text{or Au}(e_{cb}^-) + H^+ \rightarrow \text{Ag or Au} + H_2 \quad (11)$$

$$\text{Ag}(e_{cb}^-)\text{or Au}(e_{cb}^-) + O_2 \rightarrow \text{Ag or Au} + O_2^{-\bullet} + (H^+ + {}^-OH) \rightarrow HO_2^\bullet + {}^-OH \quad (12)$$

The mentioned mechanism accorded well with the experimental results; the most efficient catalyst is the SiO_2 NPs doped with Au^{3+} ions, and this is attributed to the ability of each Au^{3+} ion to consume three (e_{cb}^-) and generation of three $^\bullet$OH ions which are responsible for degradation of dye. The SiO_2 NPs doped with Ag^+ ions is less efficient due to the generation of only one $^\bullet$OH by each one Ag^+ ion as the electronegativity of gold is higher than silver.

Au NPs or Ag NPs deposited on the surface SiO_2 NPs act as electron–hole separation centers [52,53]. Thermodynamically the electrons transfer from the SiO_2 NPs conduction band to Au NPs or Ag NPs at the interface is allowed since the Fermi level of SiO_2 is higher than that of Au NPs or Ag NPs [54]. Consequently,

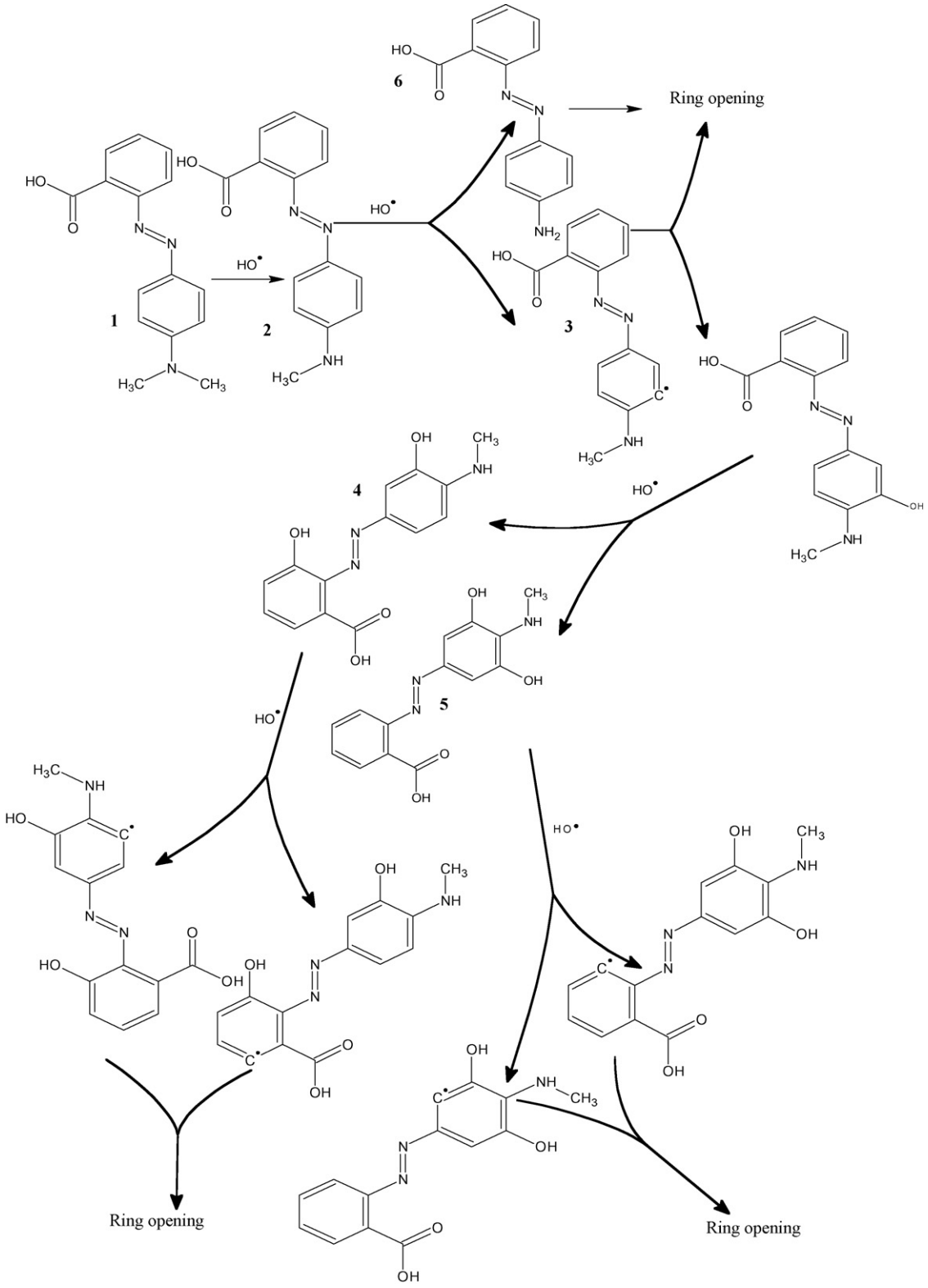

Fig. 9. Mechanism of the possible routes of the photocatalytic degradation of MR by SiO_2 NPs, (SiO_2 NPs doped with Ag^+ or Au^{3+} ions), or Ag NPs (and or) Au NPs deposited on the surface of SiO_2 NPs.

the Schottky barrier at (Au NPs or Ag NPs SiO_2 NPs) contact region was formed, which improves the charge separation and thus enhances the photocatalytic activity of SiO_2. The energy difference between the valance and conduction bands of Au NPs is lower than that in the case of Ag NPs, i.e., Ag NPs increase the activity of SiO_2 NPs more than Au NPs. The suggested electronic mechanism is illustrated in Fig. 8 and described by hydroxide attack.

The hydroxide attack might be responsible for the decolorization mechanism of the MR dye, as summarized in the schematic diagram (Fig. 9), including all the proposed steps the hydroxide radical assumed to interact with MR or intermediate photoproducts, as follows: first the •OH attack MR leading to formation of dehydrogenated radical (intermediate 2), which have two possibilities either ring opening or combination with •OH forming hydroxyl product 3. The hydroxyl product cause the broadening in the absorption spectra of the remaining MR as noticed in Fig. 3. The intermediate 2 might be also decomposed forming a new low molecular weight by-product which have absorption blue shifted in comparison with MR monomer ($\lambda_{max.} \sim 415$ nm) [55,56]. This peak which might be corresponding to the low molecular weight by-product formation was found to be increased as the rate of photocatalytic reaction decreased (decreasing the catalytic power of silica as shown in pure silica profile). The product 3 assumed to be further attacked by •OH forming bi-hydroxyl products (4 and 5) or dehydrogenated radical which undergoes ring opening. The same procedure could take place for products (4 and 5) till complete ring opening and finally mineralization.

3.7. Effect of UV irradiation on mineralization

The degradation percent of MR after photocatalytic degradation by SiO_2 NPs, SiO_2 NPs doped with Ag^+ ions, SiO_2 NPs doped with Au^{3+}ions, Ag NPs (and, or) Au NPs deposited on the surface of SiO_2 NPs catalysts are well known to be directly proportional to the following factors: (1) the lifetime of the photocatalyst because the number of active sites decreases due to contamination with by-products; (2) the rate of reaction of short aliphatic chin with •OH radicals; (3) the rate of converting the N atoms of the dye into oxidized nitrogen compounds [57]; and finally (4) the rate of formation of •OH radicals and consuming the electrons from the photocatalyst.

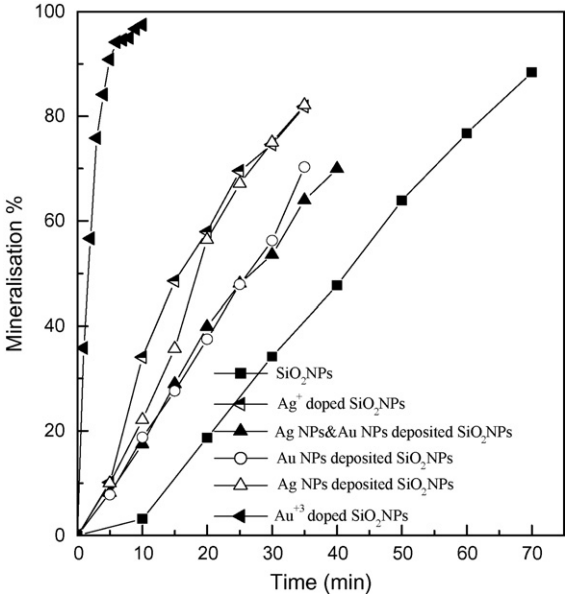

Fig. 10. The relationship between the mineralization percent of dye (MR) after the photocatalytic degradation.

Fig. 10 described the relationship between mineralization percent of MR and the photocatalytic irradiation time. To account for the amount of mineralized MR dye; the chemical oxygen demand (COD) of the remaining dye in the solution was measured. The dye was found to have mineralized to the extent of (95, 83, 85, 69, 70, 90 %) for (SiO_2 NPs doped with Au^{3+}ions, SiO_2 NPs doped with Ag^+ ions, Ag NPs deposited on SiO_2 NPs, Au NPs and Ag NPs deposited on SiO_2 NPs, Au NPs deposited on SiO_2 NPs, and SiO_2 NPs) after (10, 35, 35, 35, 40, 70 min), respectively.

References

[1] C.L. Buitron, M. Quezada, G. Moreno, Bioresour. Technol. 92 (2004) 143.
[2] M. Sokmen, D.W. Allen, F. Akkas, N. Kartal, F. Acar, Water Air Soil Pollut. 132 (2001) 153.
[3] G.T. Guyer, N.H. Lnce, Ultrason. Sonochem. 10 (2003) 235.
[4] T. Sauer, G.C. Nero, H.J. Jose, R.F.P.M. Moreira, J. Photochem. Photobiol. A Chem. 149 (2002) 147.
[5] H. Lachheb, E. Puzenat, A. Houas, M. Ksibi, E. Elaloui, C. Guillard, J.M. Herrmann, Appl. Catal. B Environ. 39 (2002) 75.
[6] Y.M. Slokar, A.M. Le Marechal, Dyes Pigments 37 (1998) 335.
[7] T. Robinson, G. McMullan, R. Marchant, P. Nigam, Bioresour. Technol. 77 (2001) 247.
[8] G. McKay, J.F. Porter, G.R. Prasad, Water Air Soil Pollut. 114 (1999) 423.
[9] N. Kannan, M. Meenakshisundaram, Water Air Soil Pollut. 138 (2002) 289.
[10] S.S. Patil, V.M. Shinde, Environ. Sci. Technol. 22 (1988) 1160.
[11] A.T. More, A. Vira, S. Fogel, Environ. Sci. Technol. 23 (1989) 403.
[12] R.H. Horning, Textile Chem. Colorist 9 (1997) 24.
[13] J. Ge, J. Qu, Appl. Catal. B Environ. 47 (2004) 133.
[14] W. Azmi, R.K. Sani, U.C. Banerjee, Enzyme Microb. Technol. 22 (1998) 185.
[15] G. Fornasari, F. Trifiro, Catal. Today 41 (1998) 443.
[16] R. Bal, B.B. Tope, T.K. Das, S.G. Hegde, S. Sivasanker, J. Catal. 204 (2001) 358.
[17] J. Haber, K. Pamin, L. Matachowski, D. Mucha, Appl. Catal. A 256 (2003) 141.
[18] A. Ogata, A. Kazusaka, M. Enyo, J. Phys. Chem. 90 (1986) 5201.
[19] Y. Inaki, H. Yoshida, T. Hattori, J. Phys. Chem. B 104 (2000) 10304.
[20] H. Yoshida, K. Kimura, Y. Inaki, T. Hattori, Chem. Commun. (1997) 129.
[21] H. Yoshida, C. Murata, T. Hattori, J. Catal. 194 (2000) 364.
[22] H. Yoshida, N. Matsushita, Y. Kato, T. Hattori, Phys. Chem. Chem. Phys. 4 (2002) 2459.
[23] H. Yoshida, Y. Kato, T. Hattori, Stud. Surf. Sci. Catal. 130 (2000) 659.
[24] H. Yoshida, M.G. Chaskar, Y. Kato, T. Hattori, Chem. Commun. (2002) 2014.
[25] Y. Kato, N. Matsushita, H. Yoshida, T. Hattori, Catal. Commun. 3 (2002) 99.
[26] Y. Inaki, H. Yoshida, T. Yoshida, T. Hattori, J. Phys. Chem. B 106 (2002) 9098.
[27] T. Furukawa, K.E. Fox, W.B. White, J. Chem. Phys. 75 (1981) 3226.
[28] L. Skuja, Optical properties of defects in silica, in: G. Pacchioni, L. Skuja, D.L. Griscom (Eds.), Defect in SiO_2 and Related Dielectrics: Science and Technology, Kluwer Academic Publishers, Netherlands, 2000, pp. 73–116.
[29] A.J. Fisher, W. Hayes, A.M. Stoneham, Phys. Rev. Lett. 64 (1990) 2667.
[30] W. Joosen, S. Guizard, P. Martin, G. Petite, P. Agostini, A.D. Santos, G. Grillon, D. Hulin, A. Migus, A. Antonetti, Appl. Phys. Lett. 61 (1992) 2260.
[31] Y. Sakurai, J. Non-Cryst. Solids 271 (2000) 218.
[32] A.J. Miller, R.G. Leisure, V.A. Mashkov, F.L. Galeener, Phys. Rev. B 53 (1996) 8818.

[33] N. San, A. Hatipoglu, G. Kocturk, Z. Cmar, J. Photochem. Photobiol. A Chem. 146 (2002) 189.
[34] U. Siemon, D. Bahnemann, J.J. Testa, D. Rodriguez, M.I. Litter, N. Bruno, J. Photochem. Photobiol. A Chem. 148 (2002) 247.
[35] B. Ohtani, K. Iwai, S. Nishimoto, S. Sato, J. Phys. Chem. B 101 (1997) 3349.
[36] H. Gerischer, A. Heller, J. Phys. Chem. 95 (1991) 5161.
[37] Z. Jiang, C. Liu, Y. Liu, Appl. Surf. Sci. 233 (2004) 153.
[38] K.V. Subba Rao, B. Lavedrine, P. Boule, J. Photochem. Photobiol. A Chem. 154 (2003) 189.
[39] P.V. Kamat, M. Flumiani, A. Dawson, Colloids Surf. A 202 (2002) 269.
[40] A. Houas, H. Lachheb, M. Ksibi, E. Elaloui, C. Guillard, J. Herrmann, Appl. Catal. B Environ. 31 (2001) 145.
[41] Z. Sun, Y. Chen, Q. Ke, Y. Yang, J. Yuan, J. Photochem. Photobiol. A Chem. 149 (2002) 169.
[42] Z.J. Jiang, C.Y. Liu, Y. Liu, Appl. Surf. Sci. 233 (2004) 135.
[43] L. Skuja, Solid State Commun. 84 (1992) 613.
[44] G. Fu, W. Cai, Y. Gan, J. Jia, Chem. Phys. Lett. 385 (2004) 15.
[45] Z.X. Yang, R.Q. Wu, D.W. Goodman, Phys. Rev. B 6 (2000) 14066.
[46] W.Z. Tang, Z. Zhang, H. An, M.O. Quintana, D.F. Torres, Environ. Technol. 18 (1997) 112.
[47] J.M. Thomas, B.F.G. Johnson, R. Raja, G. Sankar, P.A. Midgley, Acc. Chem. Res. 36 (2003) 20.
[48] V. Subramanian, E. Wolf, P.V. Kamat, J. Am. Chem. Soc. 126 (2004) 4943.
[49] T. Hirakawa, P.V. Kamat, J. Am. Chem. Soc. 127 (2005) 3928.
[50] S. Sakthivel, M.V. Shankar, M. Palanichamy, Water Res. 38 (2004) 3001.
[51] A. Linsbigler, C. Rusu, J.T. Yates, J. Am. Chem. Soc. 118 (1994) 5284.
[52] A. Henglein, J. Phys. Chem. 83 (1979) 2209.
[53] J.M. Herrmann, J. Disdier, P. Pichat, J. Phys. Chem. 90 (1986) 6028.
[54] A. Sclafani, J.M. Herrmann, J. Photochem. Photobiol. A Chem. 113 (1998) 181.
[55] R. Comparelli, E. Fanizza, M.L. Curri, P.D. Cozzoli, G. Mascolo, A. Agostiano, Appl. Catal. B Environ. 60 (2005) 1.
[56] R. Comparelli, P.D. Cozzoli, M.L. Curri, A. Agostiano, G. Mascolo, Water Sci. Tech. 49 (2004) 183.
[57] I.K. Konstantinou, T.A. Albanis, Appl. Catal. B Environ. 49 (2004) 1.